

0.1 Results: ΛK_S^0 and ΛK^\pm

In the following sections, we present results assuming (i) no residual correlations (Sec. 0.1.1), (ii) three residual contributors (Sec. 0.1.2), and (iii) ten residual contributors (Sec. 0.1.3). We find the case of three and ten contributors to be consistent, therefore we will quote the result utilizing three residuals as our final result. The results shown, unless otherwise noted, use a polynomial fit to the THERMINATOR simulation to handle the non-flat background, and $\Lambda K^+(\bar{\Lambda}K^-)$ radii are shared with $\Lambda K^-(\bar{\Lambda}K^+)$.

I first collect all of the summary results, and will show the actual fits to the data in Sections 0.1.1, 0.1.2, and 0.1.3. In the first of the summary plots, we show the extracted scattering parameters in the form of a $\text{Im}[f_0]$ vs $\text{Re}[f_0]$ plot, which includes the d_0 values to the right side. The next three summary plots show the λ vs. Radius parameters. The first group of plots shows: 1) results without any residual correlations included in the fit (marked as "QM 2017"), 2) results with 10 residual pairs included, and 3) results with 3 residual pairs included. The second group of plots also includes the case where we fixed the d_0 parameter to zero.

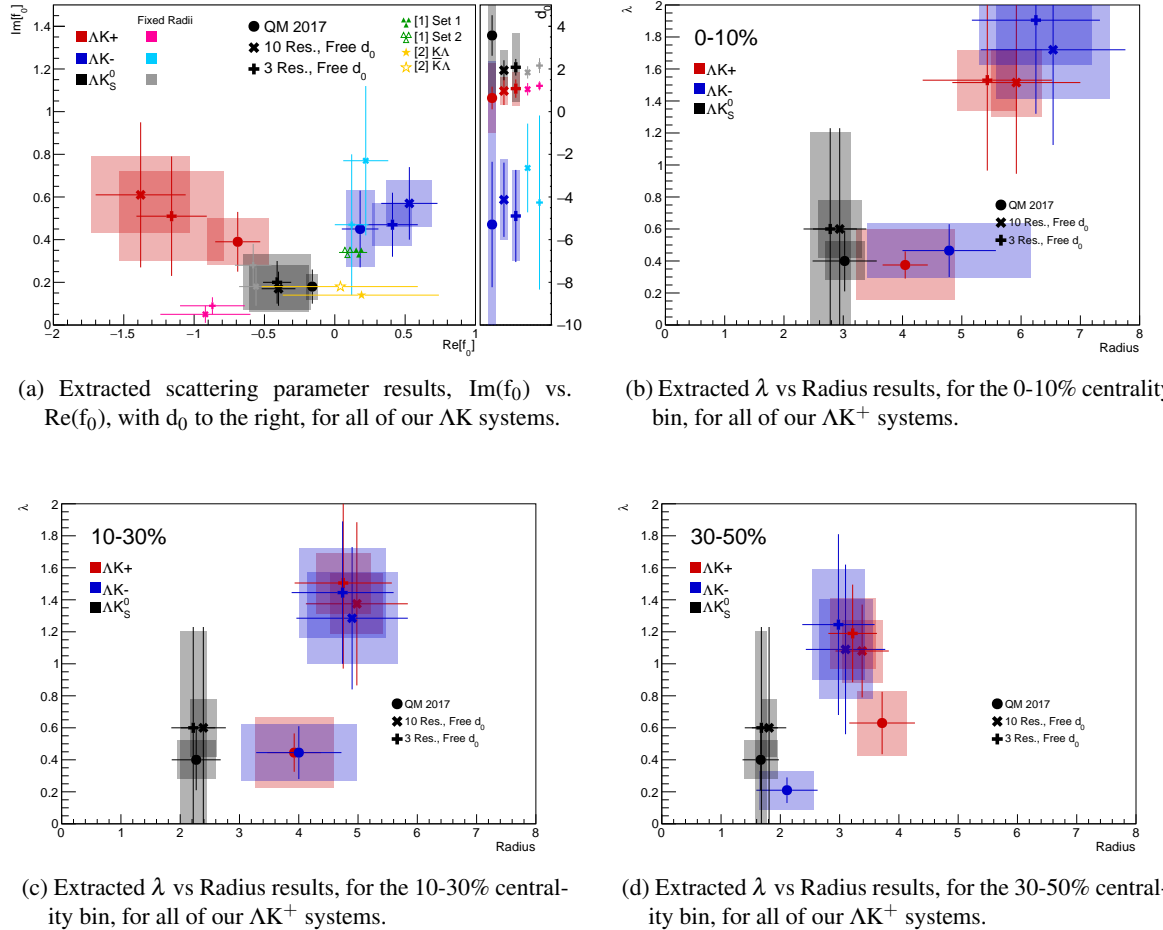


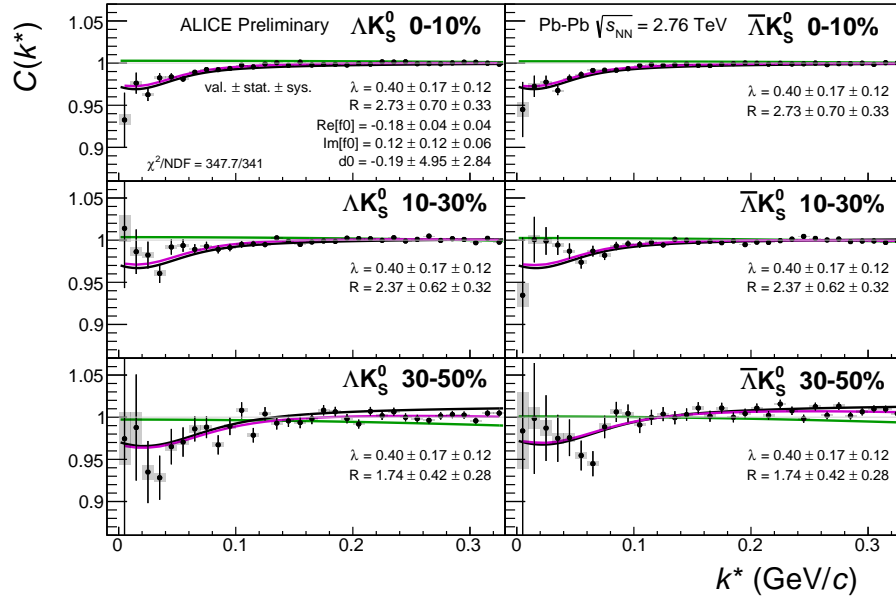
Fig. 1: Extracted fit results for all of our ΛK systems across all studied centrality bins (0-10%, 10-30%, 30-50%). The plots show results including no residuals (circles), 10 residual pairs (\times), and 3 residual pairs (+). Note, ΛK^+ on the plot is shorthand for ΛK^+ and $\bar{\Lambda}K^-$, and similar for the others. In Fig. 2a, the lighter color markers (pink, sky blue, gray) show the extracted parameters when we fix the radii to roughly align with the m_T -scaling plot (Fig. 6). Additionally, the green [?] and yellow [?] points show theoretical predictions made using chiral perturbation theory.

0.1.1 Results: ΛK_S^0 and ΛK^\pm : No Residual Correlations Included in Fit

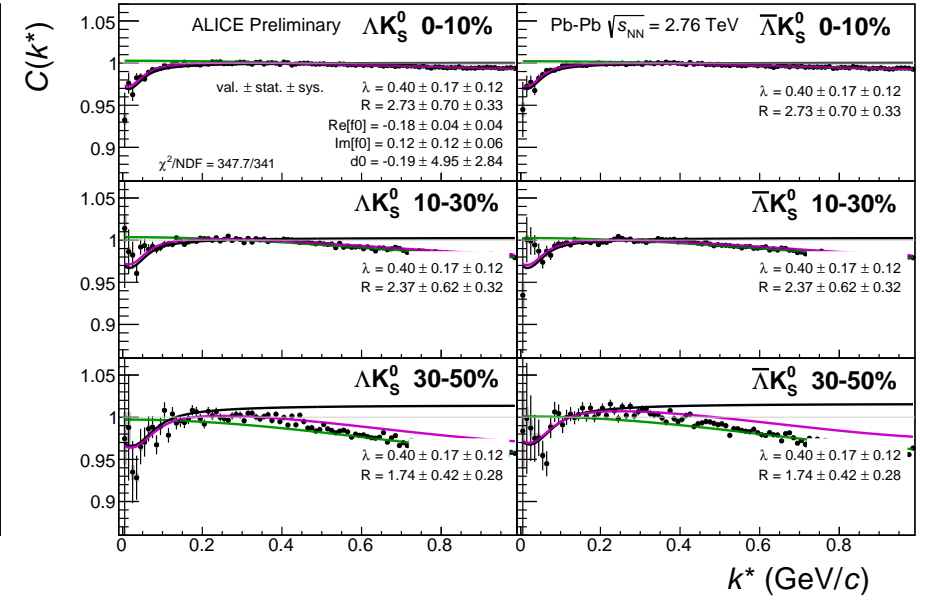
Figures 3, 4, and 5 (Section ??) show experimental data with fits for all studied centralities for ΛK_S^0 with $\bar{\Lambda} K_S^0$, ΛK^+ with $\bar{\Lambda} K^-$, and ΛK^- with $\bar{\Lambda} K^+$, respectively. The parameter sets extracted from the fits can be found in Tables ?? and ?. All correlation functions were normalized in the range $0.32 < k^* < 0.40$ GeV/c, and fit in the range $0.0 < k^* < 0.30$ GeV/c. For the ΛK^- and $\bar{\Lambda} K^+$ analyses, the region $0.19 < k^* < 0.23$ GeV/c was excluded from the fit to exclude the bump caused by the Ω^- resonance. The non-flat background was fit with a linear form from $0.6 < k^* < 0.9$ GeV/c. The theoretical fit function was then multiplied by this background during the fitting process.

In the figures (3, 4, and 5), the black solid line represents the “raw” fit, i.e. not corrected for momentum resolution effects nor non-flat background. The green line shows the fit to the non-flat background. The purple points show the fit after momentum resolution and non-flat background corrections have been applied. The initial values of the parameters is listed, as well as the final fit values with uncertainties.

For the ΛK_S^0 fits without residuals, λ was restricted to [0.4, 0.6].

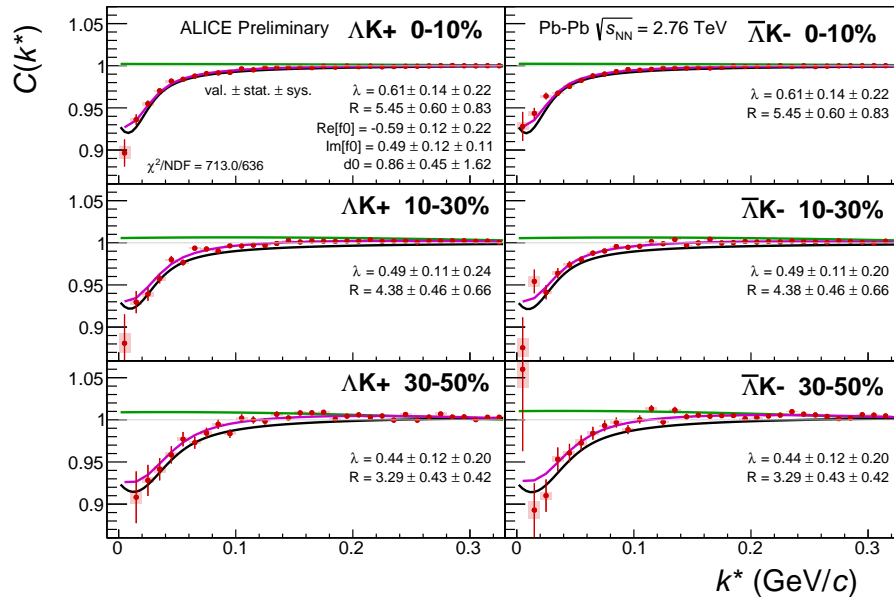


(a) Signal region view ($k^* \lesssim 0.3 \text{ GeV}/c$)

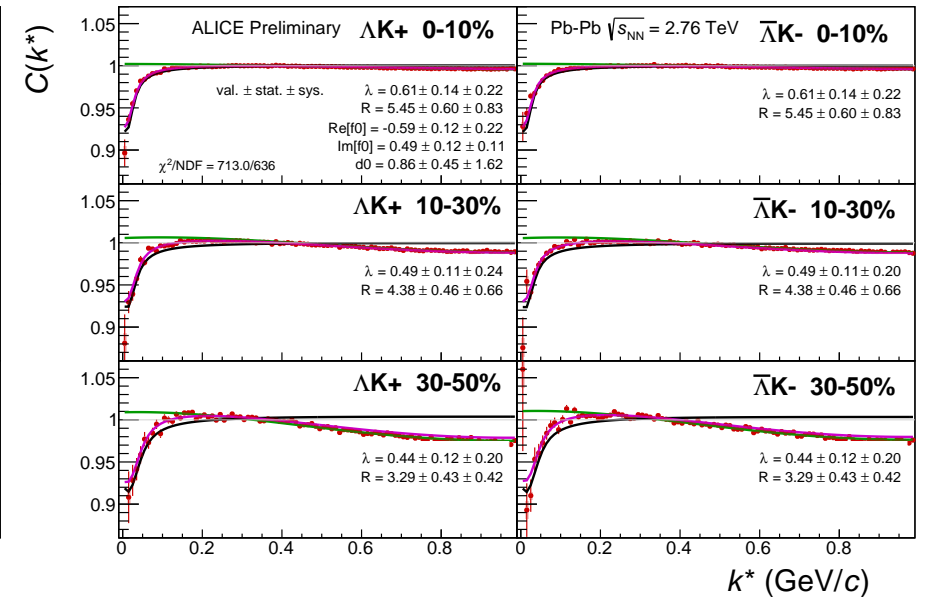


(b) Wide view ($k^* \lesssim 1.0 \text{ GeV}/c$)

Fig. 2: Fits, with NO residual correlations included, to the ΛK_s^0 (left) and $\bar{\Lambda} K_s^0$ (right) data for the centralities 0-10% (top), 10-30% (middle), and 30-50% (bottom). The lines represent the statistical errors, while the boxes represent the systematic errors. Each has unique λ and normalization parameters. The radii are shared amongst like centralities; the scattering parameters ($\mathbb{R} f_0, \mathbb{I} f_0, d_0$) are shared amongst all. The black solid line represents the “raw” fit, i.e. not corrected for momentum resolution effects nor non-flat background. The green line shows the fit to the non-flat background. The purple points show the fit after momentum resolution and non-flat background corrections have been applied. The initial values of the parameters is listed, as well as the final fit values with uncertainties. Here, R was restricted to [2.,10.] and Λ was restricted to [0.1,0.8].

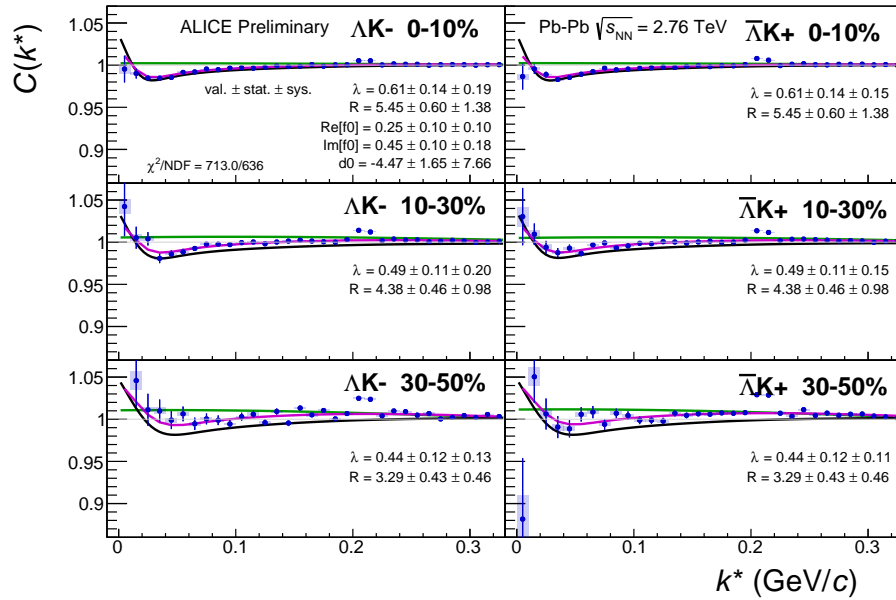


(a) Signal region view ($k^* \lesssim 0.3 \text{ GeV}/c$)

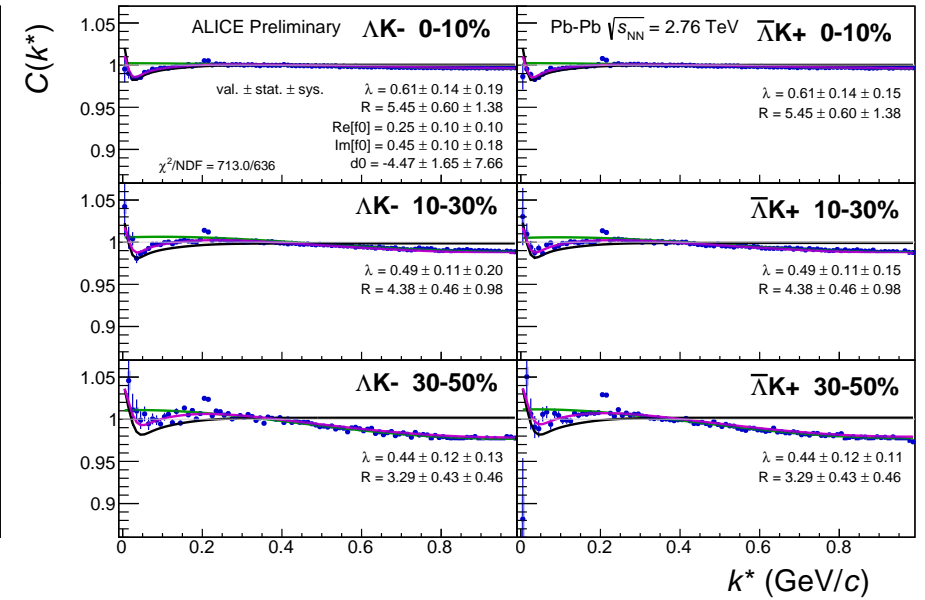


(b) Wide view ($k^* \lesssim 1.0 \text{ GeV}/c$)

Fig. 3: Fits to the ΛK^+ (left) and $\bar{\Lambda} K^-$ (right) data for the centralities 0-10% (top), 10-30% (middle), and 30-50% (bottom). The lines represent the statistical errors, while the boxes represent the systematic errors. Each has unique λ and normalization parameters. The radii are shared amongst like centralities; the scattering parameters ($\mathbb{R} f_0$, $\mathbb{I} f_0$, d_0) are shared amongst all. The black solid line represents the “raw” fit, i.e. not corrected for momentum resolution effects nor non-flat background. The green line shows the fit to the non-flat background. The purple points show the fit after momentum resolution and non-flat background corrections have been applied. The initial values of the parameters is listed, as well as the final fit values with uncertainties.



(a) Signal region view ($k^* \lesssim 0.3 \text{ GeV}/c$)



(b) Wide view ($k^* \lesssim 1.0 \text{ GeV}/c$)

Fig. 4: Fits, with NO residual correlations included, to the ΛK^- (left) with $\bar{\Lambda} K^+$ (right) data for the centralities 0-10% (top), 10-30% (middle), and 30-50% (bottom). The lines represent the statistical errors, while the boxes represent the systematic errors. Each has unique λ and normalization parameters. The radii are shared amongst like centralities; the scattering parameters ($\Re f_0, \Im f_0, d_0$) are shared amongst all. The black solid line represents the “raw” fit, i.e. not corrected for momentum resolution effects nor non-flat background. The green line shows the fit to the non-flat background. The purple points show the fit after momentum resolution and non-flat background corrections have been applied. The initial values of the parameters is listed, as well as the final fit values with uncertainties.

		Fit Results $\Lambda(\bar{\Lambda})K_S^0$				
System	Centrality	Fit Parameters				
		λ	R	$\mathbb{R}f_0$	$\mathbb{I}f_0$	d_0
$\Lambda K_S^0 \& \bar{\Lambda} K_S^0$	0-10%			2.73 ± 0.70 (stat.) ± 0.33 (sys.)		
	10-30%	0.40 ± 0.17 (stat.) ± 0.16 (sys.)	2.37 ± 0.62 (stat.) ± 0.23 (sys.)	-0.18 ± 0.04 (stat.) ± 0.16 (sys.)	0.12 ± 0.12 (stat.) ± 0.13 (sys.)	-0.19 ± 4.95 (stat.) ± 0.62 (sys.)
	30-50%			1.74 ± 0.42 (stat.) ± 0.11 (sys.)		

Table 1: Fit Results $\Lambda(\bar{\Lambda})K_S^0$, with no residual correlations included. Each pair is fit simultaneously with its conjugate (ie. ΛK_S^0 with $\bar{\Lambda} K_S^0$) across all centralities (0-10%, 10-30%, 30-50%), for a total of 6 simultaneous analyses in the fit. A single λ parameter is shared amongst all. Each analysis has a unique normalization parameter. The radii are shared between analyses of like centrality, as these should have similar source sizes. The scattering parameters ($\mathbb{R}f_0$, $\mathbb{I}f_0$, d_0) are shared amongst all. The background is modeled by a (6th-degree polynomial fit to THERMINATOR simulation. The fit is done on the data with only statistical error bars. The errors marked as “stat.” are those returned by MINUIT. The errors marked as “sys.” are those which result from my systematic analysis (as outlined in Section ??).

		Fit Results $\Lambda(\bar{\Lambda})K^\pm$					
System	Centrality	Fit Parameters					
		λ	R	$\mathbb{R}f_0$	$\mathbb{I}f_0$	d_0	
$\Lambda K^+ & \bar{\Lambda} K^-$	0-10%	0.61 ± 0.14 (stat.) ± 0.28 (sys.)	5.45 ± 0.60 (stat.) ± 0.54 (sys.)	-0.59 ± 0.12 (stat.) ± 0.36 (sys.)	0.49 ± 0.12 (stat.) ± 0.23 (sys.)	0.86 ± 0.45 (stat.) ± 0.53 (sys.)	
	10-30%	0.49 ± 0.11 (stat.) ± 0.36 (sys.)	4.38 ± 0.46 (stat.) ± 0.42 (sys.)				
$\Lambda K^+ & \bar{\Lambda} K^-$	30-50%	0.44 ± 0.12 (stat.) ± 0.31 (sys.)	3.29 ± 0.43 (stat.) ± 0.32 (sys.)	0.25 ± 0.10 (stat.) ± 0.14 (sys.)	0.45 ± 0.10 (stat.) ± 0.11 (sys.)	-4.47 ± 1.65 (stat.) ± 1.33 (sys.)	

Table 2: Fit Results $\Lambda(\bar{\Lambda})K^\pm$, with no residual correlations included. All ΛK^\pm analyses are fit simultaneously across all centralities (0-10%, 10-30%, 30-50%). Scattering parameters ($\mathbb{R}f_0$, $\mathbb{I}f_0$, d_0) are shared between pair-conjugate systems (i.e. a parameter set describing the ΛK^+ & $\bar{\Lambda} K^-$ system, and a separate set describing the ΛK^- & $\bar{\Lambda} K^+$ system). For each centrality, a radius and λ parameters are shared between all pairs (ΛK^+ , $\bar{\Lambda} K^-$, ΛK^- , $\bar{\Lambda} K^+$). Each analysis has a unique normalization parameter. The background is modeled by a (6th-)degree polynomial fit to THERMINATOR simulation. The fit is done on the data with only statistical error bars. The errors marked as “stat.” are those returned by MINUIT. The errors marked as “sys.” are those which result from my systematic analysis (as outlined in Section ??).

Figure 6 shows extracted R_{inv} parameters as a function of transverse mass (m_T) for various pair systems over several centralities. The published ALICE data [?] is shown with transparent, open symbols. The new ΛK results are shown with opaque, filled symbols. The radii show an increasing size with increasing centrality, as is expected from the simple geometric picture of the collisions. The radii decrease in size with increasing m_T , and we see an approximate scaling of the radii with transverse mass, as is expected in the presence of collective flow in the system.

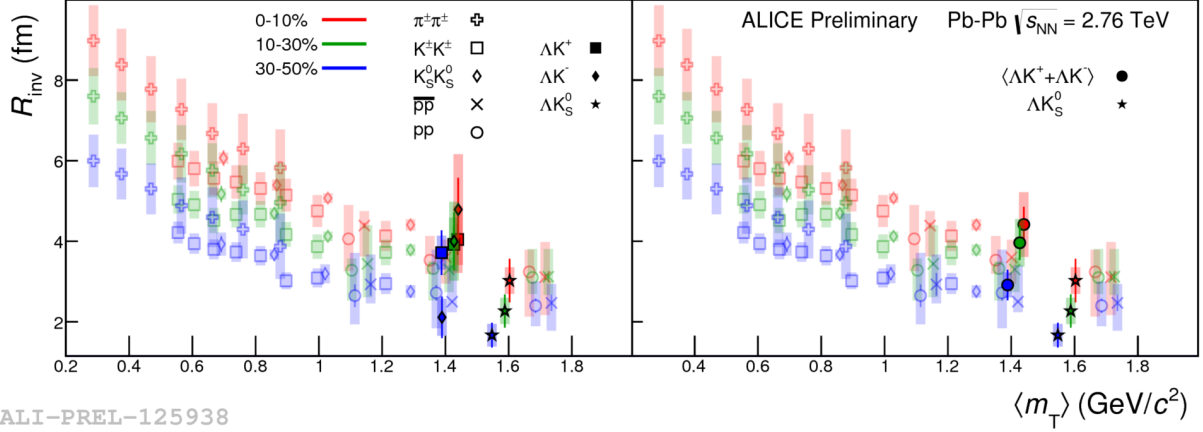


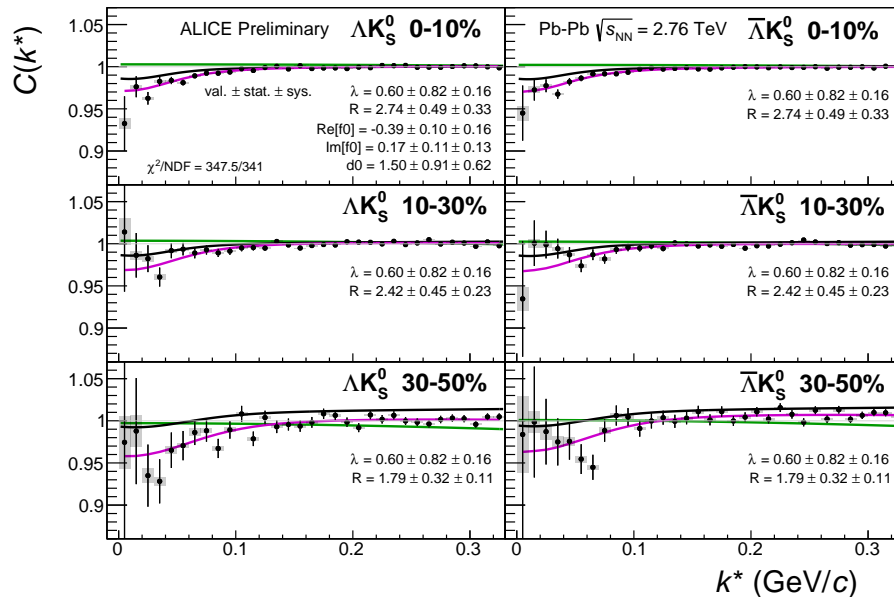
Fig. 5: No residual correlations in ΛK fits. Extracted fit R_{inv} parameters as a function of pair transverse mass (m_T) for various pair systems over several centralities. The ALICE published data [?] is shown with transparent, open symbols. The new ΛK results are shown with opaque, filled symbols. In the left, the ΛK^+ (with its conjugate pair) results are shown separately from the ΛK^- (with its conjugate pair) results. In the right, all ΛK^\pm results are averaged.

0.1.2 Results: ΛK_S^0 and ΛK^\pm : 3 Residual Correlations Included in Fit

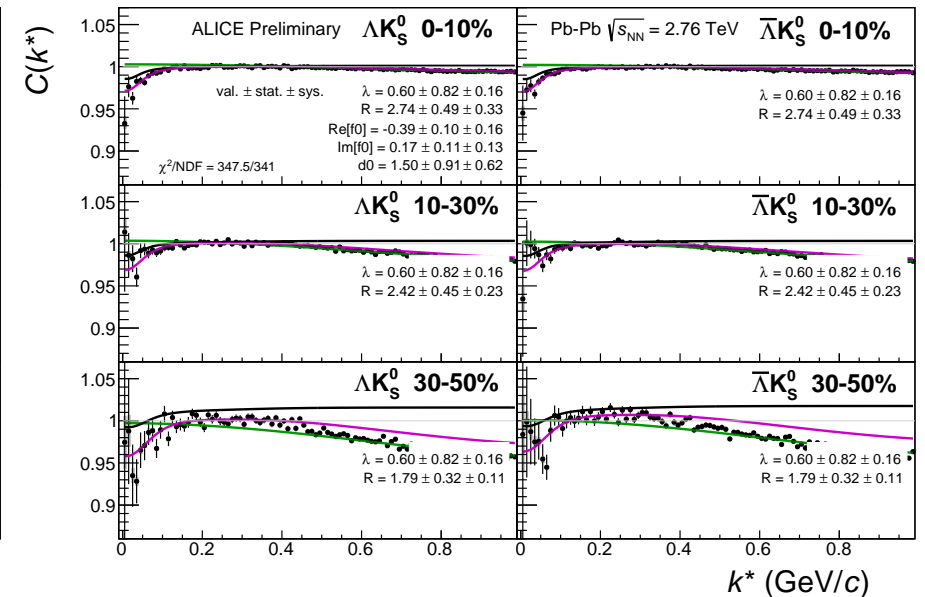
Figures 7, 8, and 9 (Section ??) show experimental data with fits for all studied centralities for ΛK_S^0 with $\bar{\Lambda} K_S^0$, ΛK^+ with $\bar{\Lambda} K^-$, and ΛK^- with $\bar{\Lambda} K^+$, respectively. The parameter sets extracted from the fits can be found in Tables 5 and 6. All correlation functions were normalized in the range $0.32 < k^* < 0.40$ GeV/c, and fit in the range $0.0 < k^* < 0.30$ GeV/c. For the ΛK^- and $\bar{\Lambda} K^+$ analyses, the region $0.19 < k^* < 0.23$ GeV/c was excluded from the fit to exclude the bump caused by the Ω^- resonance. The non-flat background was fit with a linear form from $0.6 < k^* < 0.9$ GeV/c. The theoretical fit function was then multiplied by this background during the fitting process.

In the figures (7, 8, and 9), the black solid line represents the “raw” fit, i.e. not corrected for momentum resolution effects nor non-flat background. The green line shows the fit to the non-flat background. The purple points show the fit after momentum resolution and non-flat background corrections have been applied. The initial values of the parameters is listed, as well as the final fit values with uncertainties.

For the ΛK_S^0 fits without residuals, λ was restricted to [0.4, 0.6].

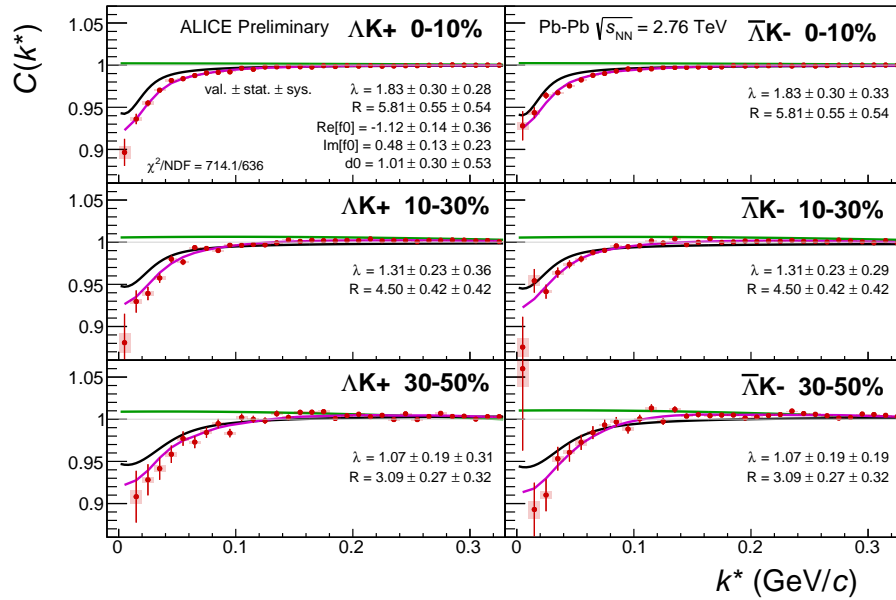


(a) Signal region view ($k^* \lesssim 0.3$ GeV/c)

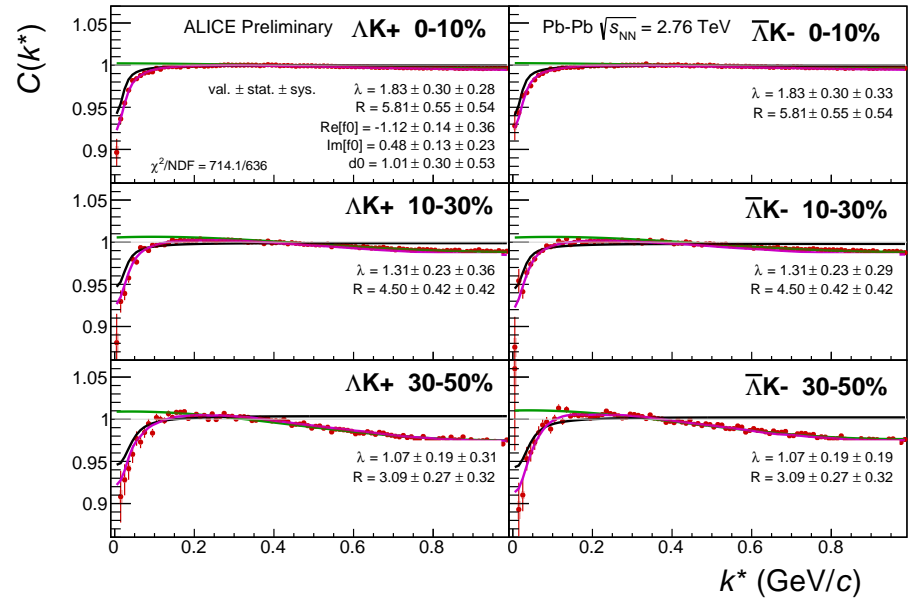


(b) Wide view ($k^* \lesssim 1.0$ GeV/c)

Fig. 6: Fits, with 3 residual correlations included, to the ΛK_s^0 (left) and $\bar{\Lambda} K_s^0$ (right) data for the centralities 0-10% (top), 10-30% (middle), and 30-50% (bottom). The lines represent the statistical errors, while the boxes represent the systematic errors. Each has unique λ and normalization parameters. The radii are shared amongst like centralities; the scattering parameters ($\mathbb{R} f_0$, $\mathbb{I} f_0$, d_0) are shared amongst all. The black solid line represents the “raw” fit, i.e. not corrected for momentum resolution effects nor non-flat background. The green line shows the fit to the non-flat background. The purple points show the fit after momentum resolution and non-flat background corrections have been applied. The initial values of the parameters is listed, as well as the final fit values with uncertainties. Here, R was restricted to [2.,10.] and λ was restricted to [0.1,0.8].

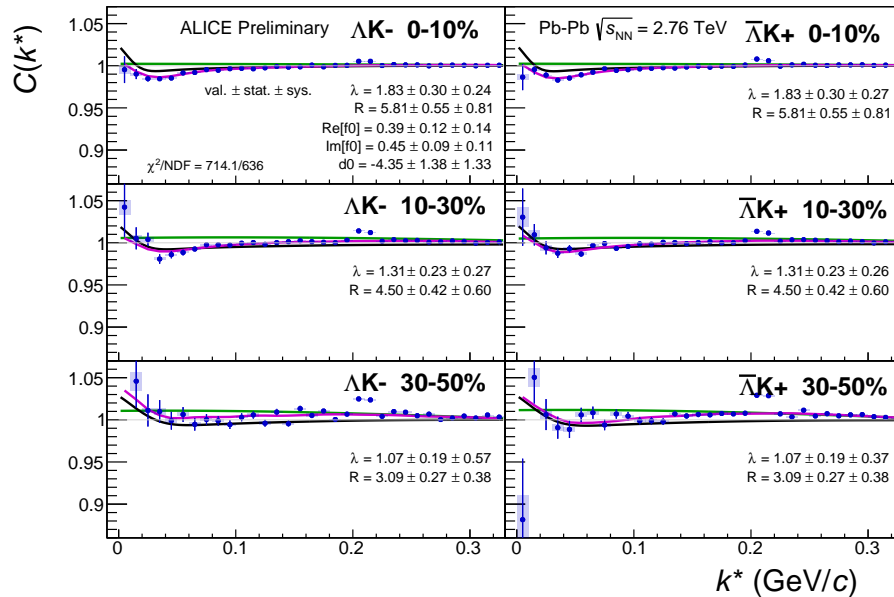


(a) Signal region view ($k^* \lesssim 0.3 \text{ GeV}/c$)

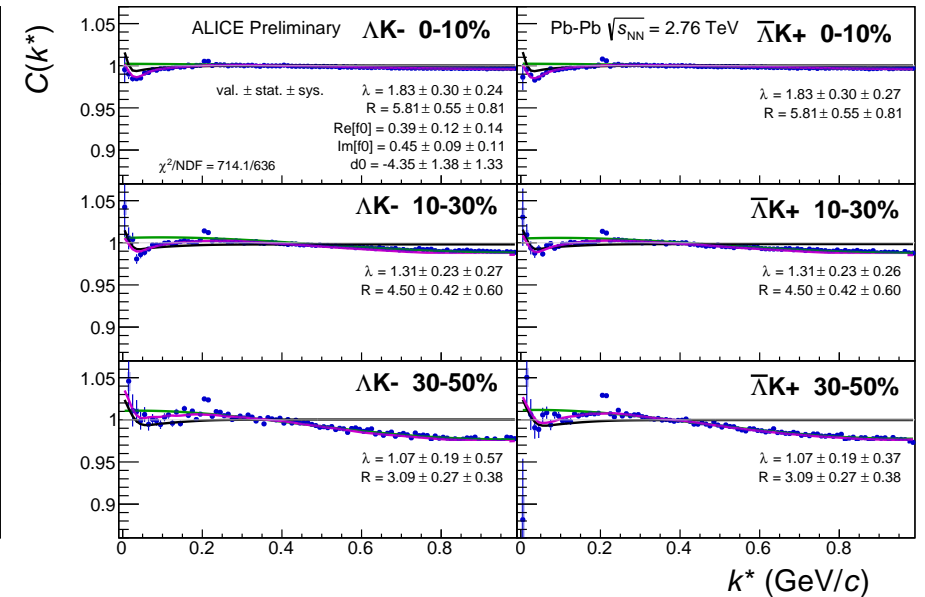


(b) Wide view ($k^* \lesssim 1.0 \text{ GeV}/c$)

Fig. 7: Fits, with 3 residual correlations included, to the ΛK^+ (left) and $\bar{\Lambda} K^-$ (right) data for the centralities 0-10% (top), 10-30% (middle), and 30-50% (bottom). The lines represent the statistical errors, while the boxes represent the systematic errors. Each has unique λ and normalization parameters. The radii are shared amongst like centralities; the scattering parameters ($\Re f_0, \Im f_0, d_0$) are shared amongst all. The black solid line represents the “raw” fit, i.e. not corrected for momentum resolution effects nor non-flat background. The green line shows the fit to the non-flat background. The purple points show the fit after momentum resolution and non-flat background corrections have been applied. The initial values of the parameters is listed, as well as the final fit values with uncertainties.



(a) Signal region view ($k^* \lesssim 0.3 \text{ GeV}/c$)



(b) Wide view ($k^* \lesssim 1.0 \text{ GeV}/c$)

Fig. 8: Fits, with 3 residual correlations included, to the ΛK^- (left) with $\bar{\Lambda} K^+$ (right) data for the centralities 0-10% (top), 10-30% (middle), and 30-50% (bottom). The lines represent the statistical errors, while the boxes represent the systematic errors. Each has unique λ and normalization parameters. The radii are shared amongst like centralities; the scattering parameters ($\mathbb{R}f_0, \mathbb{I}f_0, d_0$) are shared amongst all. The black solid line represents the “raw” fit, i.e. not corrected for momentum resolution effects nor non-flat background. The green line shows the fit to the non-flat background. The purple points show the fit after momentum resolution and non-flat background corrections have been applied. The initial values of the parameters is listed, as well as the final fit values with uncertainties.

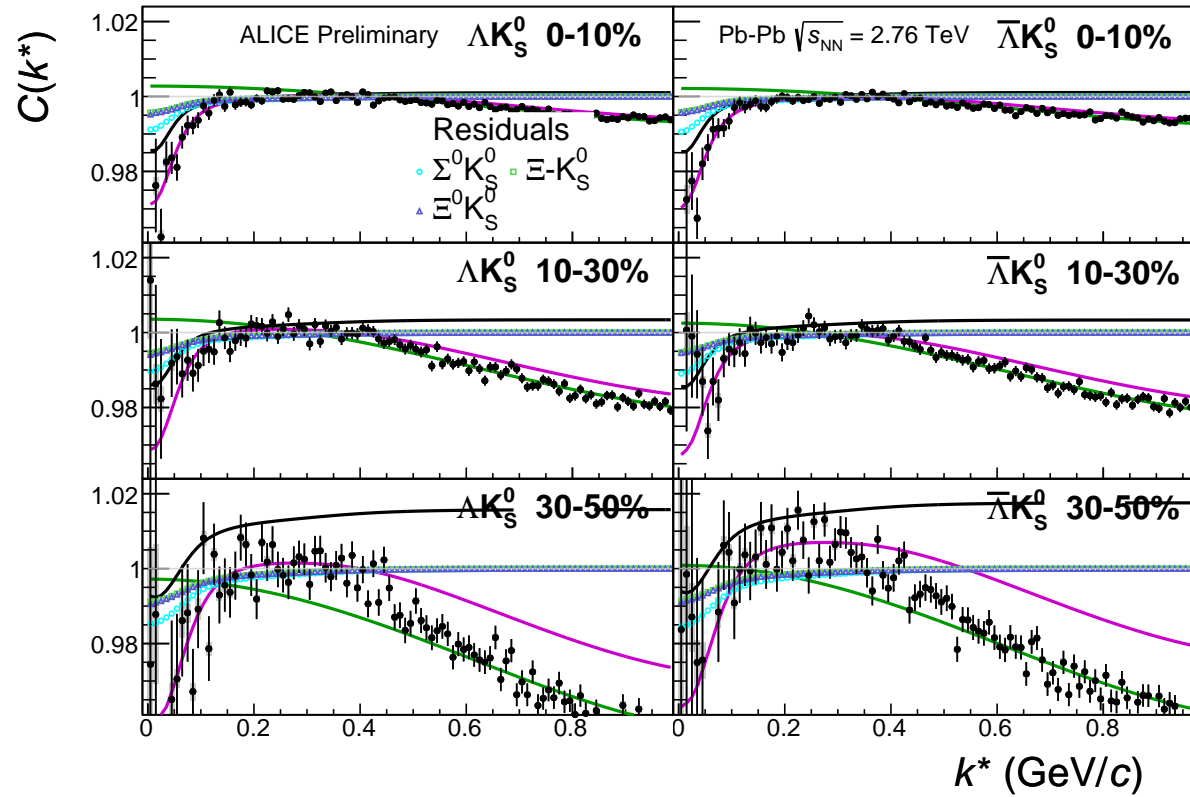
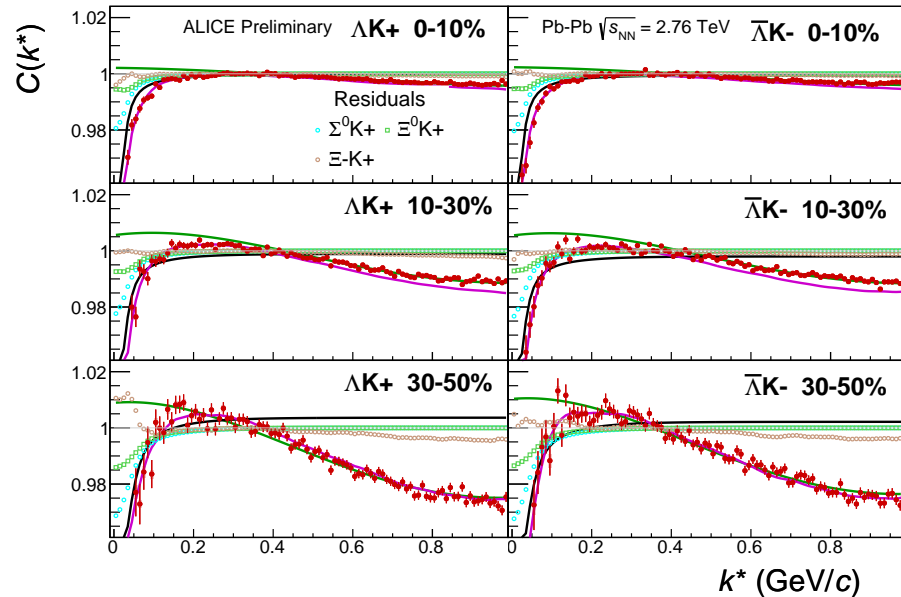
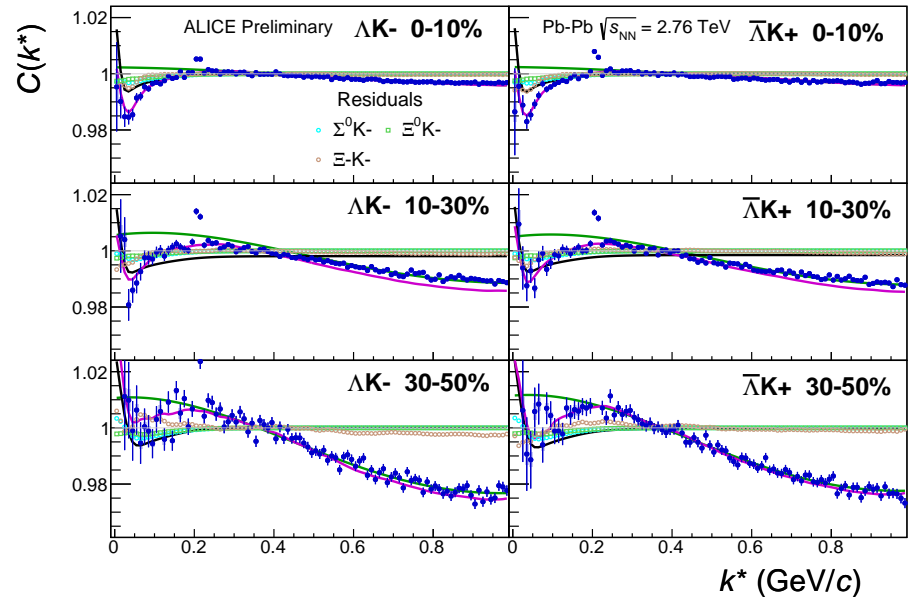


Fig. 9: Fits, with 3 residual correlations included and shown, to the ΛK_S^0 (left) and $\bar{\Lambda} K_S^0$ (right) data for the centralities 0-10% (top), 10-30% (middle), and 30-50% (bottom). The three parent pairs used for the residual correction to the ΛK_S^0 ($\bar{\Lambda} K_S^0$) fit are $\Sigma^0 K_S^0$, $\Xi^0 K_S^0$, and $\Xi^- K_S^0$ ($\bar{\Sigma}^0 K_S^0$, $\bar{\Xi}^0 K_S^0$, and $\bar{\Xi}^+ K_S^0$).



(a) ΛK^+ ($\bar{\Lambda} K^-$) fits with residual contributions shown for the centralities 0-10% (top), 10-30% (middle), and 30-50% (bottom)



(b) ΛK^- ($\bar{\Lambda} K^+$) fits with residual contributions shown for the centralities 0-10% (top), 10-30% (middle), and 30-50% (bottom)

Fig. 10: Fits, with 3 residual correlations included and shown, to the ΛK^+ & $\bar{\Lambda} K^-$ (left) and ΛK^- & $\bar{\Lambda} K^+$ (right) data for the centralities 0-10% (top), 10-30% (middle), and 30-50% (bottom). The three parent pairs used for the residual correction to the ΛK^+ ($\bar{\Lambda} K^-$) fit are $\Sigma^0 K^+$, $\Xi^0 K^+$, and $\Xi^- K^-$ ($\bar{\Sigma}^0 K^-$, $\bar{\Xi}^0 K^-$, and $\bar{\Xi}^+ K^-$).

Fit Results $\Lambda(\bar{\Lambda})K_S^0$						
System	Centrality	Fit Parameters				
		λ	R	$\mathbb{R}f_0$	$\mathbb{I}f_0$	d_0
$\Lambda K_S^0 \text{ & } \bar{\Lambda} K_S^0$	0-10%	$0.60 \pm 0.82 \text{ (stat.)} \pm 0.16 \text{ (sys.)}$	$2.74 \pm 0.49 \text{ (stat.)} \pm 0.33 \text{ (sys.)}$	$-0.39 \pm 0.10 \text{ (stat.)} \pm 0.16 \text{ (sys.)}$	$0.17 \pm 0.11 \text{ (stat.)} \pm 0.13 \text{ (sys.)}$	$1.50 \pm 0.91 \text{ (stat.)} \pm 0.62 \text{ (sys.)}$
	10-30%		$2.42 \pm 0.45 \text{ (stat.)} \pm 0.23 \text{ (sys.)}$			
	30-50%		$1.79 \pm 0.32 \text{ (stat.)} \pm 0.11 \text{ (sys.)}$			

Table 3: Fit Results $\Lambda(\bar{\Lambda})K_S^0$, with 3 residual correlations included. Each pair is fit simultaneously with its conjugate (ie. ΛK_S^0 with $\bar{\Lambda} K_S^0$) across all centralities (0-10%, 10-30%, 30-50%), for a total of 6 simultaneous analyses in the fit. A single λ parameter is shared amongst all. Each analysis has a unique normalization parameter. The radii are shared between analyses of like centrality, as these should have similar source sizes. The scattering parameters ($\mathbb{R}f_0$, $\mathbb{I}f_0$, d_0) are shared amongst all. The background is modeled by a (6th-)degree polynomial fit to THERMINATOR simulation. The fit is done on the data with only statistical error bars. The errors marked as “stat.” are those returned by MINUIT. The errors marked as “sys.” are those which result from my systematic analysis (as outlined in Section ??).

		Fit Results $\Lambda(\bar{\Lambda})K^\pm$				
System	Centrality	Fit Parameters				
		λ	R	$\mathbb{R}f_0$	$\mathbb{I}f_0$	d_0
$\Lambda K^+ & \bar{\Lambda} K^-$	0-10%	1.83 ± 0.30 (stat.) ± 0.28 (sys.)	5.81 ± 0.55 (stat.) ± 0.54 (sys.)	-1.12 ± 0.14 (stat.) ± 0.36 (sys.)	0.48 ± 0.13 (stat.) ± 0.23 (sys.)	1.01 ± 0.30 (stat.) ± 0.53 (sys.)
	10-30%	1.31 ± 0.23 (stat.) ± 0.36 (sys.)	4.50 ± 0.42 (stat.) ± 0.42 (sys.)			
$\Lambda K^+ & \bar{\Lambda} K^-$	30-50%	1.07 ± 0.19 (stat.) ± 0.31 (sys.)	3.09 ± 0.27 (stat.) ± 0.32 (sys.)	0.39 ± 0.12 (stat.) ± 0.14 (sys.)	0.45 ± 0.09 (stat.) ± 0.11 (sys.)	-4.35 ± 1.38 (stat.) ± 1.33 (sys.)

Table 4: Fit Results $\Lambda(\bar{\Lambda})K^\pm$, with 3 residual correlations included. All ΛK^\pm analyses are fit simultaneously across all centralities (0-10%, 10-30%, 30-50%). Scattering parameters ($\mathbb{R}f_0$, $\mathbb{I}f_0$, d_0) are shared between pair-conjugate systems (i.e. a parameter set describing the $\Lambda K^+ & \bar{\Lambda} K^-$ system, and a separate set describing the $\Lambda K^- & \bar{\Lambda} K^+$ system). For each centrality, a radius and λ parameters are shared between all pairs ($\Lambda K^+, \bar{\Lambda} K^-, \Lambda K^-, \bar{\Lambda} K^+$). Each analysis has a unique normalization parameter. The background is modeled by a (6th-)degree polynomial fit to THERMINATOR simulation. The fit is done on the data with only statistical error bars. The errors marked as “stat.” are those returned by MINUIT. The errors marked as “sys.” are those which result from my systematic analysis (as outlined in Section ??).

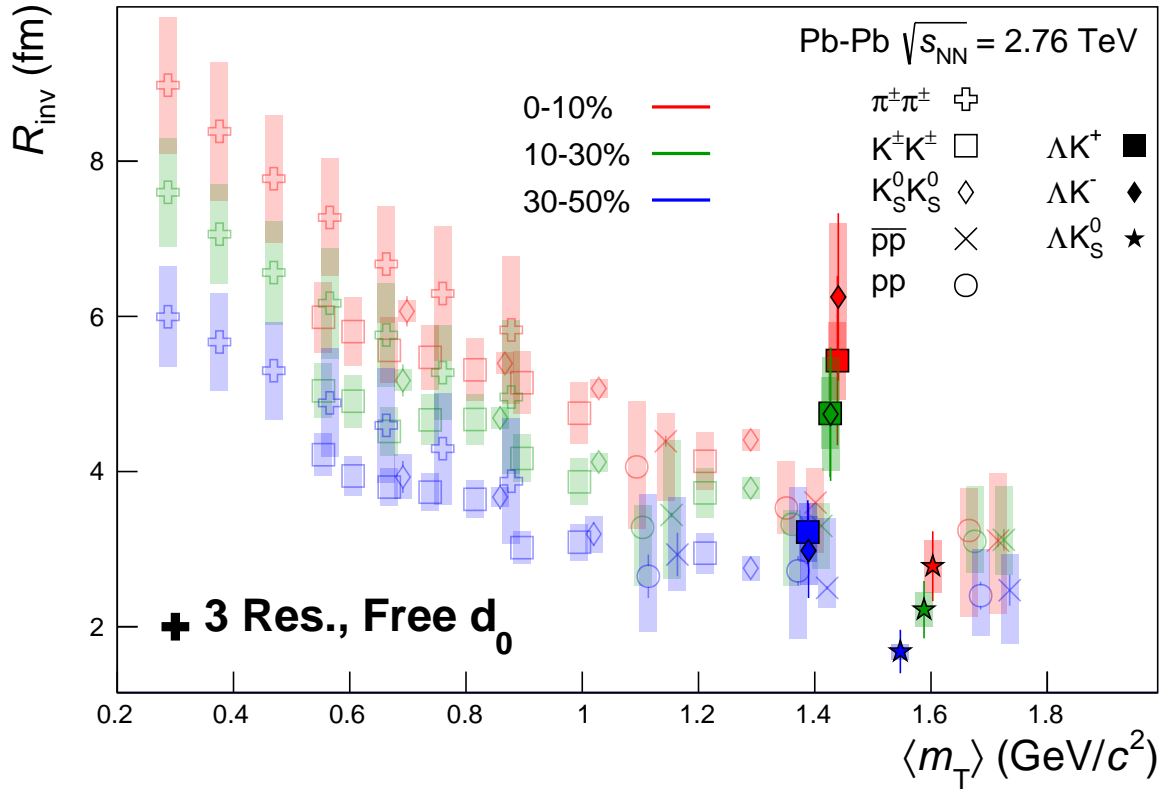


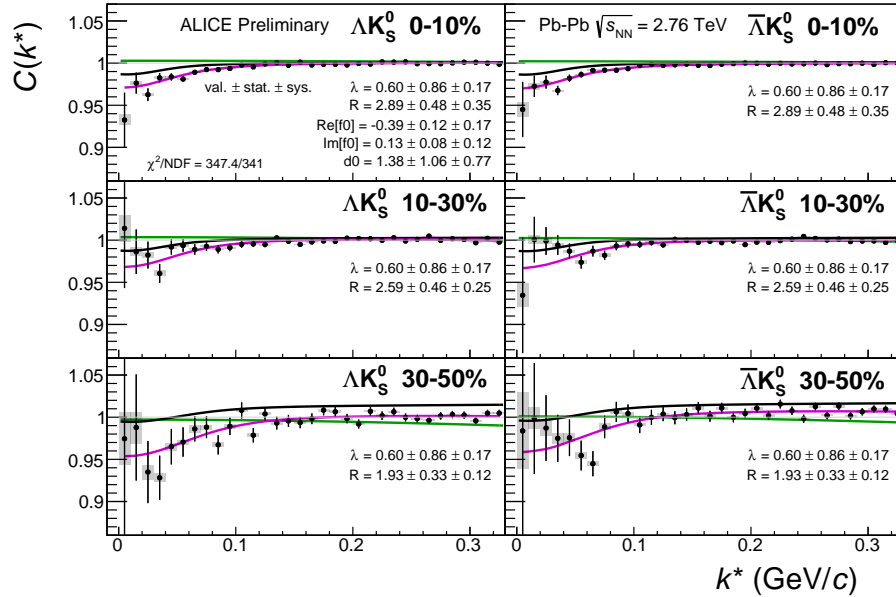
Fig. 11: 3 residual correlations in ΛK fits. Extracted fit R_{inv} parameters as a function of pair transverse mass (m_T) for various pair systems over several centralities. The ALICE published data [?] is shown with transparent, open symbols. The new ΛK results are shown with opaque, filled symbols. In the left, the ΛK^+ (with its conjugate pair) results are shown separately from the ΛK^- (with its conjugate pair) results. In the right, all ΛK^\pm results are averaged.

0.1.3 Results: ΛK_S^0 and ΛK^\pm : 10 Residual Correlations Included in Fit

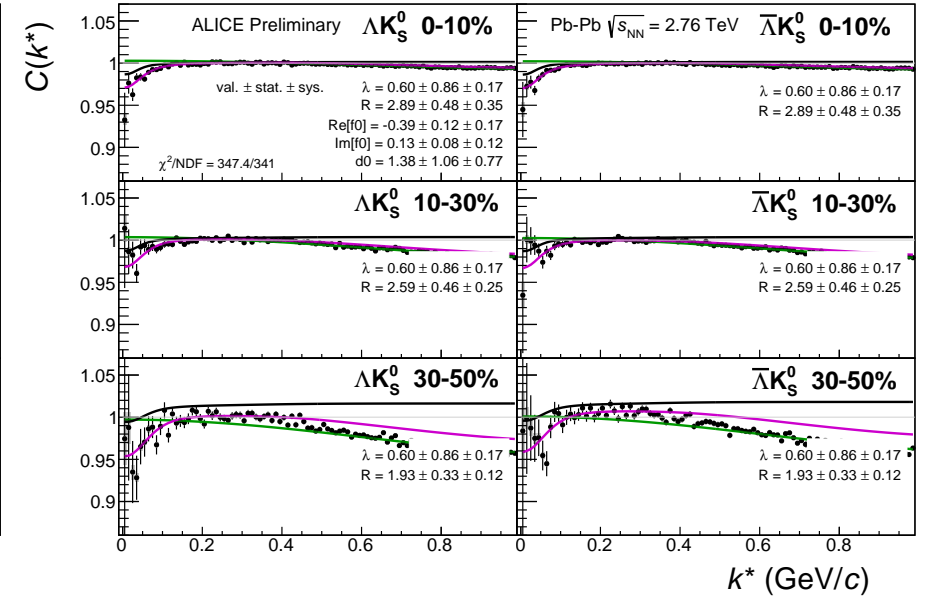
Figures 13, 14, and 15 (Section ??) show experimental data with fits for all studied centralities for ΛK_S^0 with $\bar{\Lambda} K_S^0$, ΛK^+ with $\bar{\Lambda} K^-$, and ΛK^- with $\bar{\Lambda} K^+$, respectively. The parameter sets extracted from the fits can be found in Tables ?? and ???. All correlation functions were normalized in the range $0.32 < k^* < 0.40$ GeV/c, and fit in the range $0.0 < k^* < 0.30$ GeV/c. For the ΛK^- and $\bar{\Lambda} K^+$ analyses, the region $0.19 < k^* < 0.23$ GeV/c was excluded from the fit to exclude the bump caused by the Ω^- resonance. The non-flat background was fit with a linear form from $0.6 < k^* < 0.9$ GeV/c. The theoretical fit function was then multiplied by this background during the fitting process.

In the figures (13, 14, and 15), the black solid line represents the “raw” fit, i.e. not corrected for momentum resolution effects nor non-flat background. The green line shows the fit to the non-flat background. The purple points show the fit after momentum resolution and non-flat background corrections have been applied. The initial values of the parameters is listed, as well as the final fit values with uncertainties.

For the ΛK_S^0 fits without residuals, λ was restricted to [0.4, 0.6].

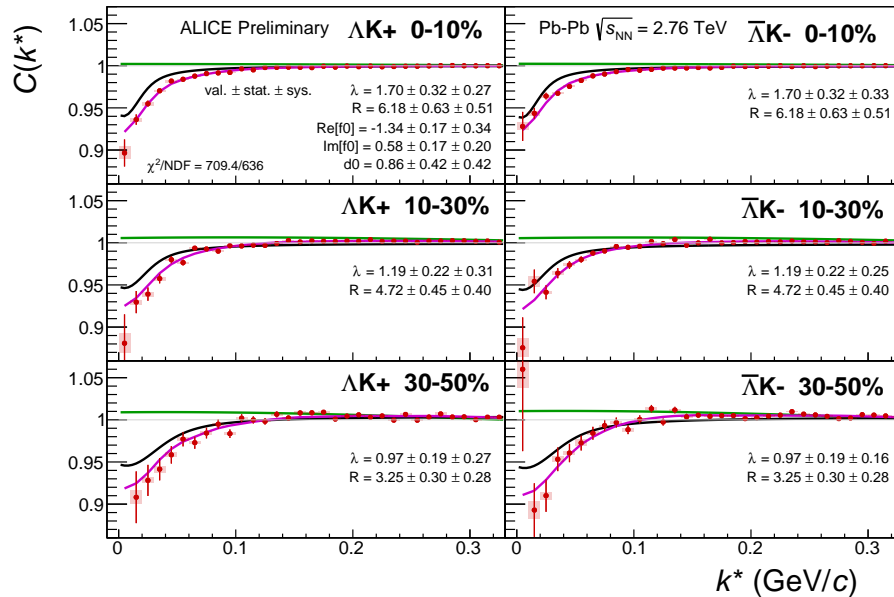


(a) Signal region view ($k^* \lesssim 0.3 \text{ GeV}/c$)

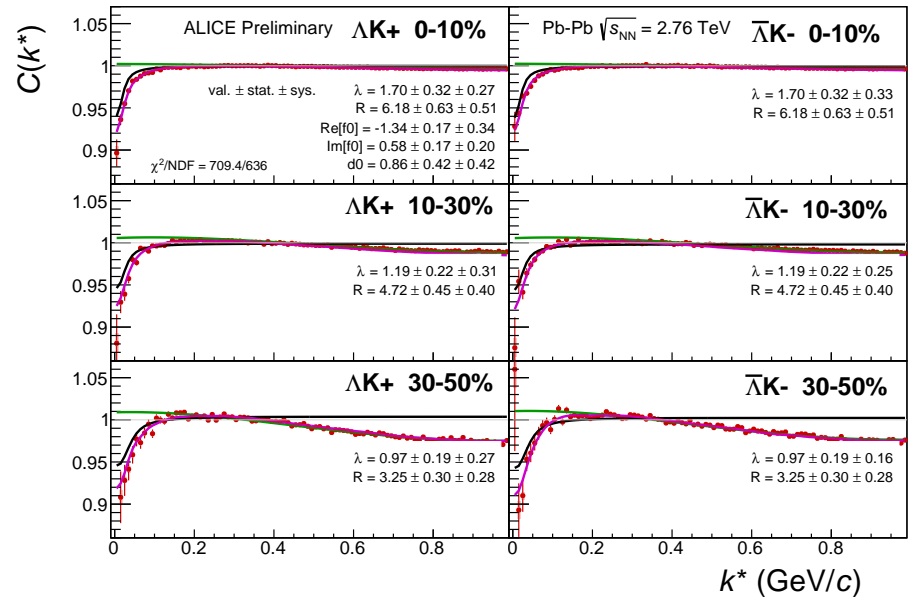


(b) Wide view ($k^* \lesssim 1.0 \text{ GeV}/c$)

Fig. 12: Fits, with 10 residual correlations included, to the ΛK_s^0 (left) and $\bar{\Lambda} K_s^0$ (right) data for the centralities 0-10% (top), 10-30% (middle), and 30-50% (bottom). The lines represent the statistical errors, while the boxes represent the systematic errors. Each has unique λ and normalization parameters. The radii are shared amongst like centralities; the scattering parameters ($\mathbb{R} f_0, \mathbb{I} f_0, d_0$) are shared amongst all. The black solid line represents the “raw” fit, i.e. not corrected for momentum resolution effects nor non-flat background. The green line shows the fit to the non-flat background. The purple points show the fit after momentum resolution and non-flat background corrections have been applied. The initial values of the parameters is listed, as well as the final fit values with uncertainties. Here, R was restricted to [2.,10.] and Λ was restricted to [0.1,0.8].

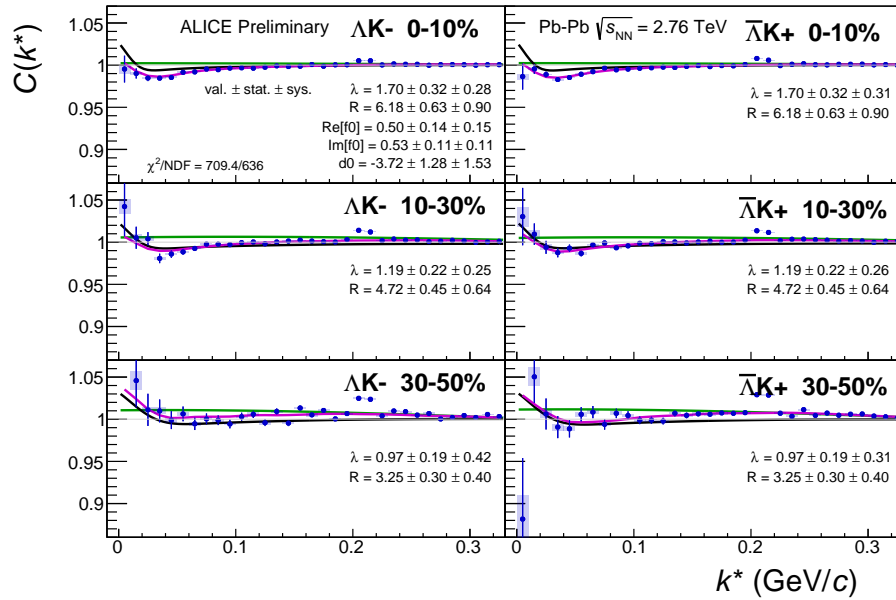


(a) Signal region view ($k^* \lesssim 0.3 \text{ GeV}/c$)

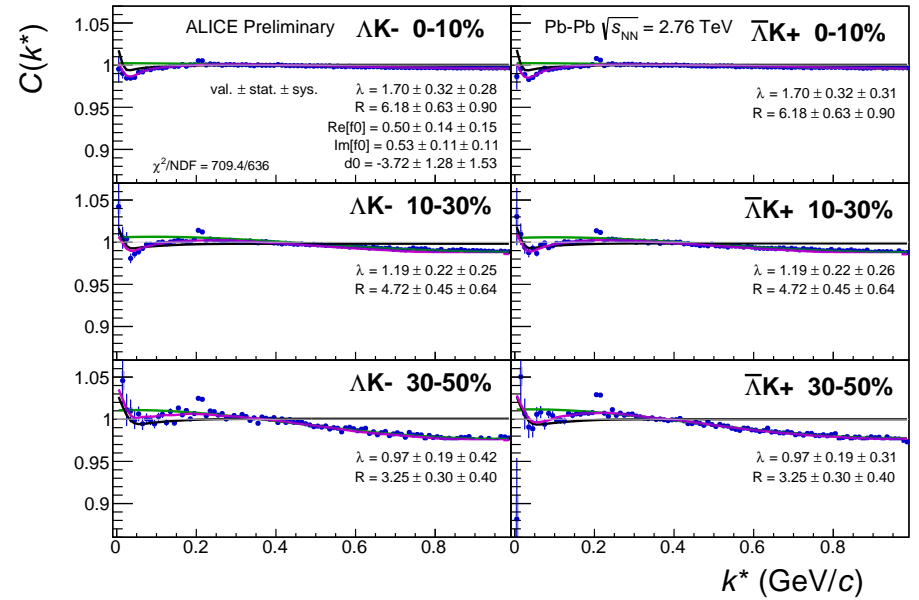


(b) Wide view ($k^* \lesssim 1.0 \text{ GeV}/c$)

Fig. 13: Fits, with 10 residual correlations included, to the ΛK^+ (left) and $\bar{\Lambda} K^-$ (right) data for the centralities 0-10% (top), 10-30% (middle), and 30-50% (bottom). The lines represent the statistical errors, while the boxes represent the systematic errors. Each has unique λ and normalization parameters. The radii are shared amongst like centralities; the scattering parameters ($Re[f_0]$, $Im[f_0]$, d_0) are shared amongst all. The black solid line represents the “raw” fit, i.e. not corrected for momentum resolution effects nor non-flat background. The green line shows the fit to the non-flat background. The purple points show the fit after momentum resolution and non-flat background corrections have been applied. The initial values of the parameters is listed, as well as the final fit values with uncertainties.



(a) Signal region view ($k^* \lesssim 0.3 \text{ GeV}/c$)



(b) Wide view ($k^* \lesssim 1.0 \text{ GeV}/c$)

Fig. 14: Fits, with 10 residual correlations included, to the ΛK^- (left) with $\bar{\Lambda} K^+$ (right) data for the centralities 0-10% (top), 10-30% (middle), and 30-50% (bottom). The lines represent the statistical errors, while the boxes represent the systematic errors. Each has unique λ and normalization parameters. The radii are shared amongst like centralities; the scattering parameters ($\text{Re}[f_0]$, $\text{Im}[f_0]$, d_0) are shared amongst all. The black solid line represents the “raw” fit, i.e. not corrected for momentum resolution effects nor non-flat background. The green line shows the fit to the non-flat background. The purple points show the fit after momentum resolution and non-flat background corrections have been applied. The initial values of the parameters is listed, as well as the final fit values with uncertainties.

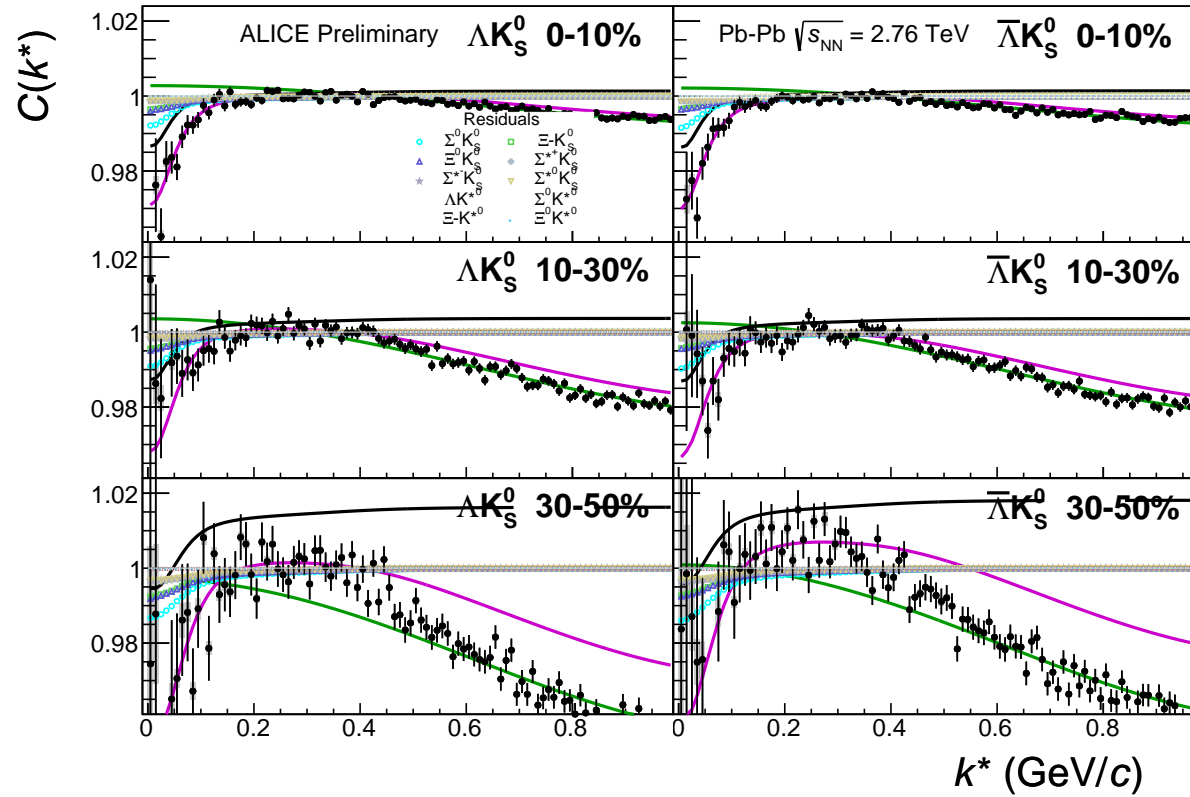
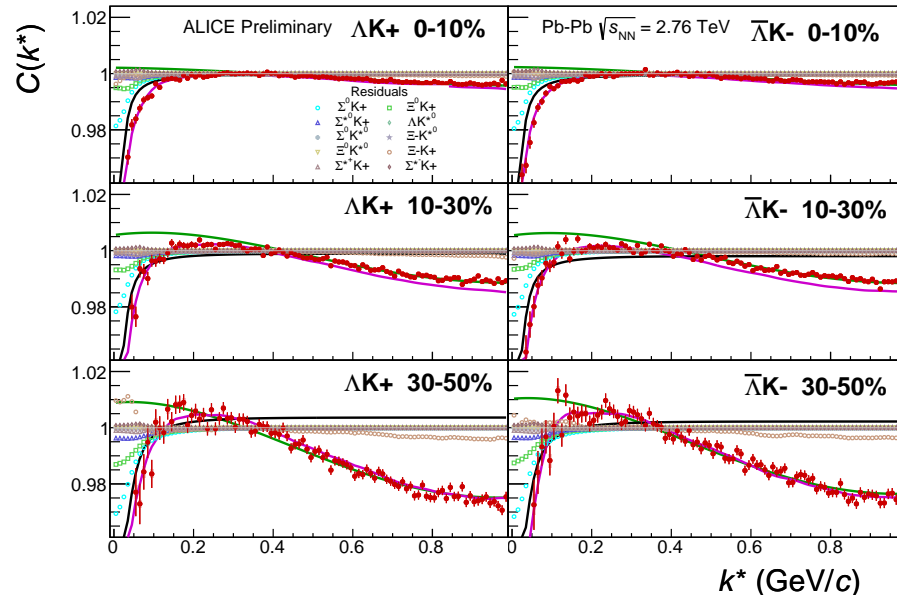
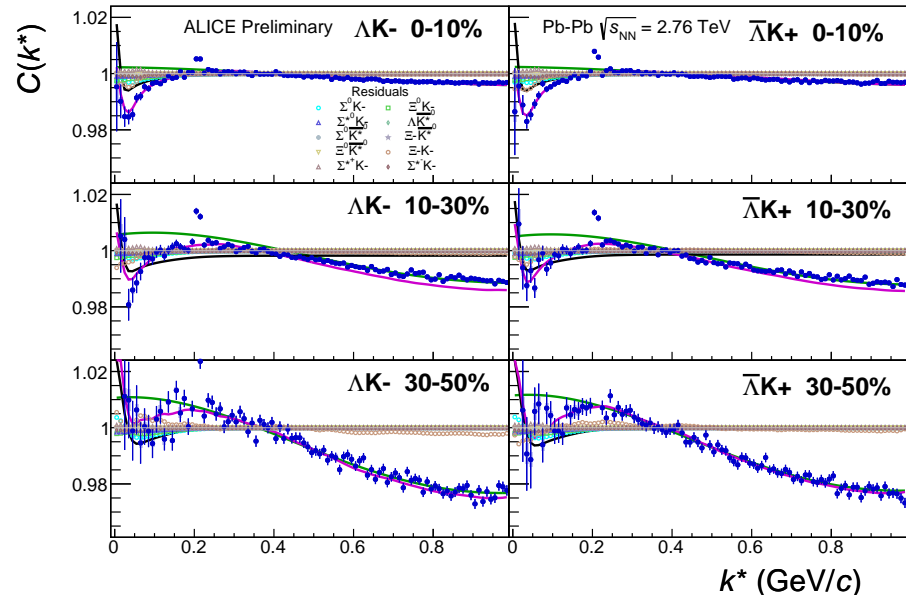


Fig. 15: Fits, with 10 residual correlations included and shown, to the ΛK_S^0 (left) and $\bar{\Lambda} K_S^0$ (right) data for the centralities 0-10% (top), 10-30% (middle), and 30-50% (bottom). The ten parent pairs used for the residual correction to the ΛK_S^0 ($\bar{\Lambda} K_S^0$) fit are $\Sigma^0 K_S^0$, $\Xi^0 K_S^0$, $\Xi^- K_S^0$, $\Sigma^{(+,-,0)} K_S^0$, ΛK^{*0} , $\Sigma^0 K^{*0}$, $\Xi^0 K^{*0}$, and $\Xi^- K^{*0}$ ($\bar{\Sigma}^0 K_S^0$, $\bar{\Xi}^0 K_S^0$, $\bar{\Xi}^+ K_S^0$, $\bar{\Sigma}^{(+,-,0)} K_S^0$, $\bar{\Lambda} K^{*0}$, $\bar{\Sigma}^0 \bar{K}^{*0}$, $\bar{\Xi}^0 \bar{K}^{*0}$, and $\bar{\Xi}^+ \bar{K}^{*0}$).



(a) $\Lambda K^+(\bar{\Lambda} K^-)$ fits with residual contributions shown for the centralities 0-10% (top), 10-30% (middle), and 30-50% (bottom)



(b) $\Lambda K^- (\bar{\Lambda} K^+)$ fits with residual contributions shown for the centralities 0-10% (top), 10-30% (middle), and 30-50% (bottom)

Fig. 16: Fits, with 10 residual correlations included and shown, to the ΛK^+ & $\bar{\Lambda} K^-$ (left) and ΛK^- & $\bar{\Lambda} K^+$ (right) data for the centralities 0-10% (top), 10-30% (middle), and 30-50% (bottom). The ten parent pairs used for the residual correction to the ΛK^+ ($\bar{\Lambda} K^-$) fit are $\Sigma^0 K^+$, $\Xi^0 K^+$, $\Xi^- K^+$, $\Sigma^{*(+,-,0)} K^+$, ΛK^{*0} , $\Sigma^0 K^{*0}$, $\Xi^0 K^{*0}$, and $\Xi^- K^{*0}$ ($\bar{\Sigma}^0 K^-$, $\bar{\Xi}^0 K^-$, $\bar{\Xi}^+ K^-$, $\bar{\Sigma}^{*(+,-,0)} K^-$, $\bar{\Lambda} \bar{K}^{*0}$, $\bar{\Sigma}^0 \bar{K}^{*0}$, $\bar{\Xi}^0 \bar{K}^{*0}$, and $\bar{\Xi}^+ \bar{K}^{*0}$).

		Fit Results $\Lambda(\bar{\Lambda})K_S^0$				
System	Centrality	Fit Parameters				
		λ	R	$\mathbb{R}f_0$	$\mathbb{I}f_0$	d_0
$\Lambda K_S^0 \& \bar{\Lambda} K_S^0$	0-10%		2.89 ± 0.48 (stat.) ± 0.33 (sys.)			
	10-30%	0.60 ± 0.86 (stat.) ± 0.16 (sys.)	2.59 ± 0.46 (stat.) ± 0.23 (sys.)	-0.39 ± 0.12 (stat.) ± 0.16 (sys.)	0.13 ± 0.08 (stat.) ± 0.13 (sys.)	1.38 ± 1.06 (stat.) ± 0.62 (sys.)
	30-50%		1.93 ± 0.33 (stat.) ± 0.11 (sys.)			

Table 5: Fit Results $\Lambda(\bar{\Lambda})K_S^0$, with 10 residual correlations included. Each pair is fit simultaneously with its conjugate (ie. ΛK_S^0 with $\bar{\Lambda} K_S^0$) across all centralities (0-10%, 10-30%, 30-50%), for a total of 6 simultaneous analyses in the fit. A single λ parameter is shared amongst all. Each analysis has a unique normalization parameter. The radii are shared between analyses of like centrality, as these should have similar source sizes. The scattering parameters ($\mathbb{R}f_0$, $\mathbb{I}f_0$, d_0) are shared amongst all. The background is modeled by a (6th-degree polynomial fit to THERMINATOR simulation. The fit is done on the data with only statistical error bars. The errors marked as “stat.” are those returned by MINUIT. The errors marked as “sys.” are those which result from my systematic analysis (as outlined in Section ??).

		Fit Results $\Lambda(\bar{\Lambda})K^\pm$					
System	Centrality	Fit Parameters					
		λ	R	$\mathbb{R}f_0$	$\mathbb{I}f_0$	d_0	
$\Lambda K^+ & \bar{\Lambda} K^-$	0-10%	1.70 ± 0.32 (stat.) ± 0.28 (sys.)	6.18 ± 0.63 (stat.) ± 0.54 (sys.)	-1.34 ± 0.17 (stat.) ± 0.36 (sys.)	0.58 ± 0.17 (stat.) ± 0.23 (sys.)	0.86 ± 0.42 (stat.) ± 0.53 (sys.)	
	10-30%	1.19 ± 0.22 (stat.) ± 0.36 (sys.)	4.72 ± 0.45 (stat.) ± 0.42 (sys.)				
$\Lambda K^+ & \bar{\Lambda} K^-$	30-50%	0.97 ± 0.19 (stat.) ± 0.31 (sys.)	3.25 ± 0.30 (stat.) ± 0.32 (sys.)	0.50 ± 0.14 (stat.) ± 0.14 (sys.)	0.53 ± 0.11 (stat.) ± 0.11 (sys.)	-3.72 ± 1.28 (stat.) ± 1.33 (sys.)	

Table 6: Fit Results $\Lambda(\bar{\Lambda})K^\pm$, with 10 residual correlations included. All ΛK^\pm analyses are fit simultaneously across all centralities (0-10%, 10-30%, 30-50%). Scattering parameters ($\mathbb{R}f_0$, $\mathbb{I}f_0$, d_0) are shared between pair-conjugate systems (i.e. a parameter set describing the ΛK^+ & $\bar{\Lambda} K^-$ system, and a separate set describing the ΛK^- & $\bar{\Lambda} K^+$ system). For each centrality, a radius and λ parameters are shared between all pairs (ΛK^+ , $\bar{\Lambda} K^-$, ΛK^- , $\bar{\Lambda} K^+$). Each analysis has a unique normalization parameter. The background is modeled by a (6th-)degree polynomial fit to THERMINATOR simulation. The fit is done on the data with only statistical error bars. The errors marked as “stat.” are those returned by MINUIT. The errors marked as “sys.” are those which result from my systematic analysis (as outlined in Section ??).

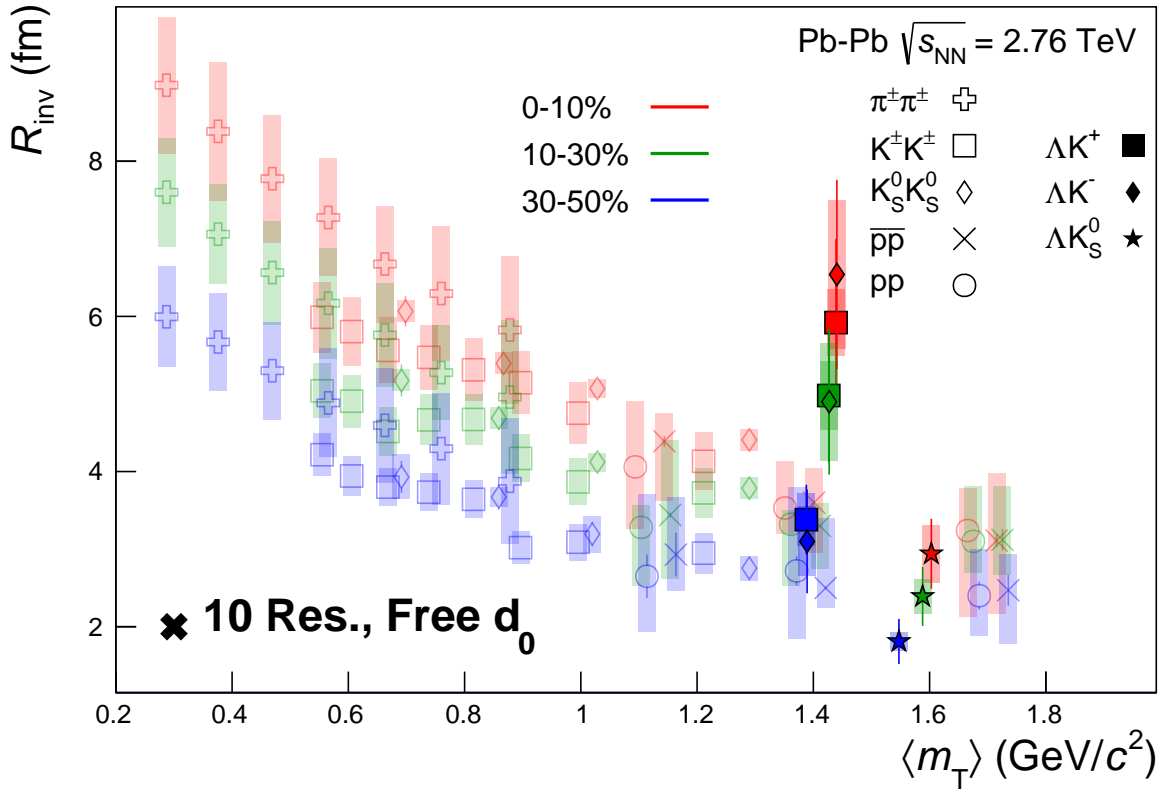


Fig. 17: 10 residual correlations in ΛK fits. Extracted fit R_{inv} parameters as a function of pair transverse mass (m_T) for various pair systems over several centralities. The ALICE published data [?] is shown with transparent, open symbols. The new ΛK results are shown with opaque, filled symbols. In the left, the ΛK^+ (with it's conjugate pair) results are shown separately from the ΛK^- (with it's conjugate pair) results. In the right, all ΛK^\pm results are averaged.

0.1.4 Results: ΛK_S^0 and ΛK^\pm : Fit Method Comparisons

In Figure 1, we show extracted fit parameters for the case of $\Lambda K^+(\bar{\Lambda}K^-)$ sharing radii with $\Lambda K^-(\bar{\Lambda}K^+)$. The figure shows results for three different treatments of the non-femtoscopic background: a polynomial fit to THERMINATOR 2 simulation to model the background (circles), a linear fit to the data to model the background (squares), and the Stavinsky method (crosses).

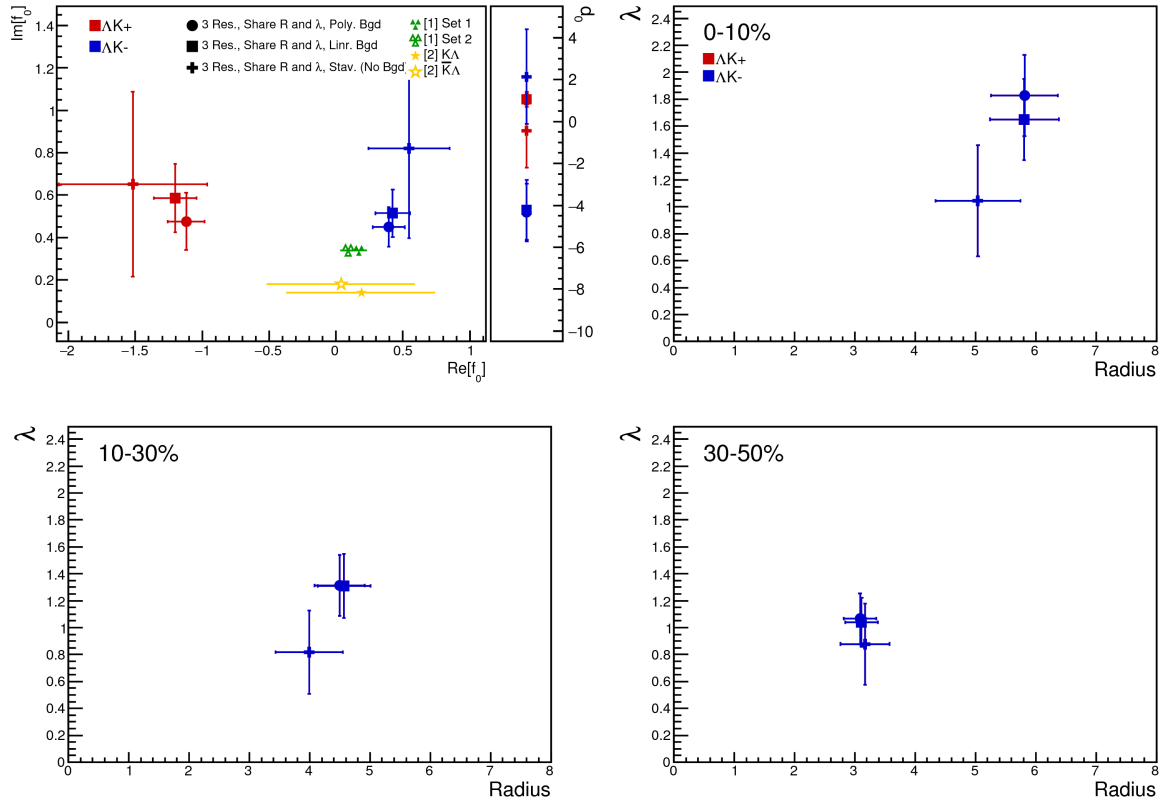


Fig. 18: Extracted fit results for all of our $\Lambda(\bar{\Lambda})K^\pm$ systems across all studied centrality bins (0-10%, 10-30%, 30-50%). The $\Lambda K^+(\bar{\Lambda}K^-)$ and $\Lambda K^-(\bar{\Lambda}K^+)$ systems share both a radius and a λ parameter for each centrality bin (i.e. 3 total radius parameters, 3 total λ parameters). The figure shows results for three different treatments of the non-femtoscopic background: a polynomial fit to THERMINATOR 2 simulation to model the background (circles), a linear fit to the data to model the background (squares), and the Stavinsky method (crosses). Note, ΛK^+ on the plot is shorthand for ΛK^+ and $\bar{\Lambda}K^- (\Lambda^+(\bar{\Lambda}K^-))$, and similar for the others. The green [?] and yellow [?] points show theoretical predictions made using chiral perturbation theory.

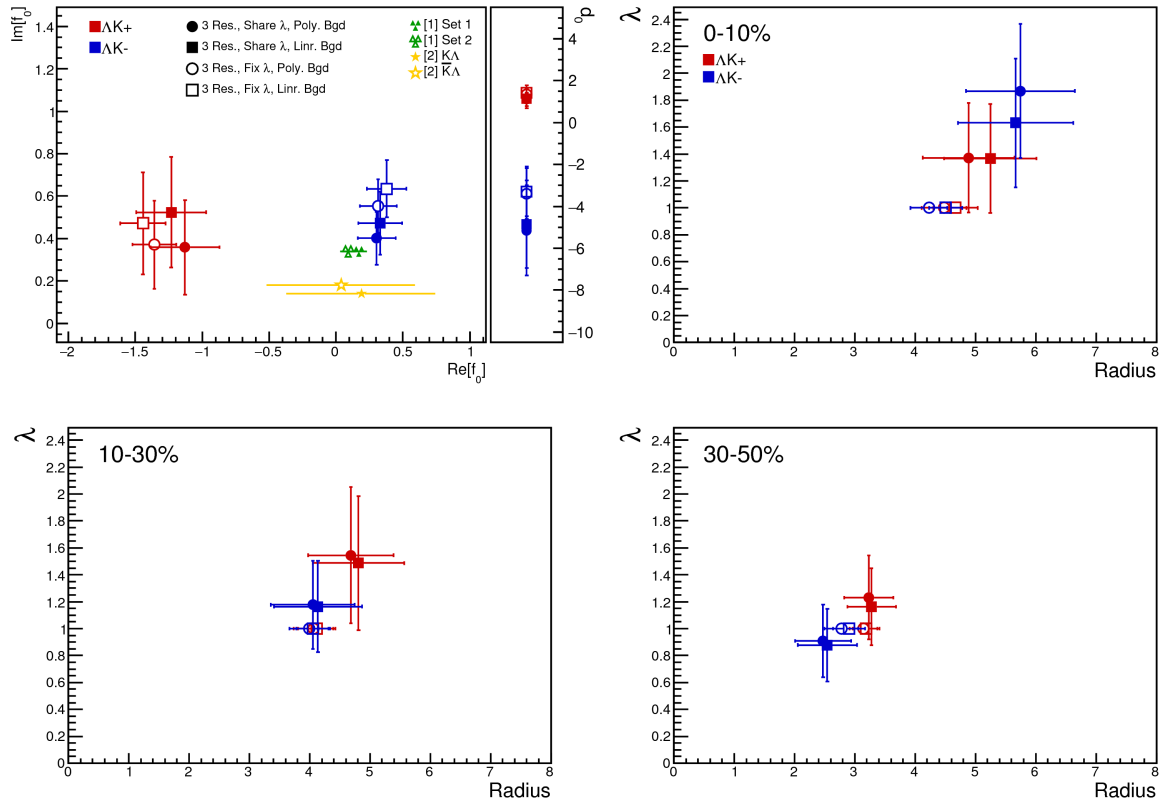


Fig. 19: Compare Fit Parameters: Free vs fixed λ

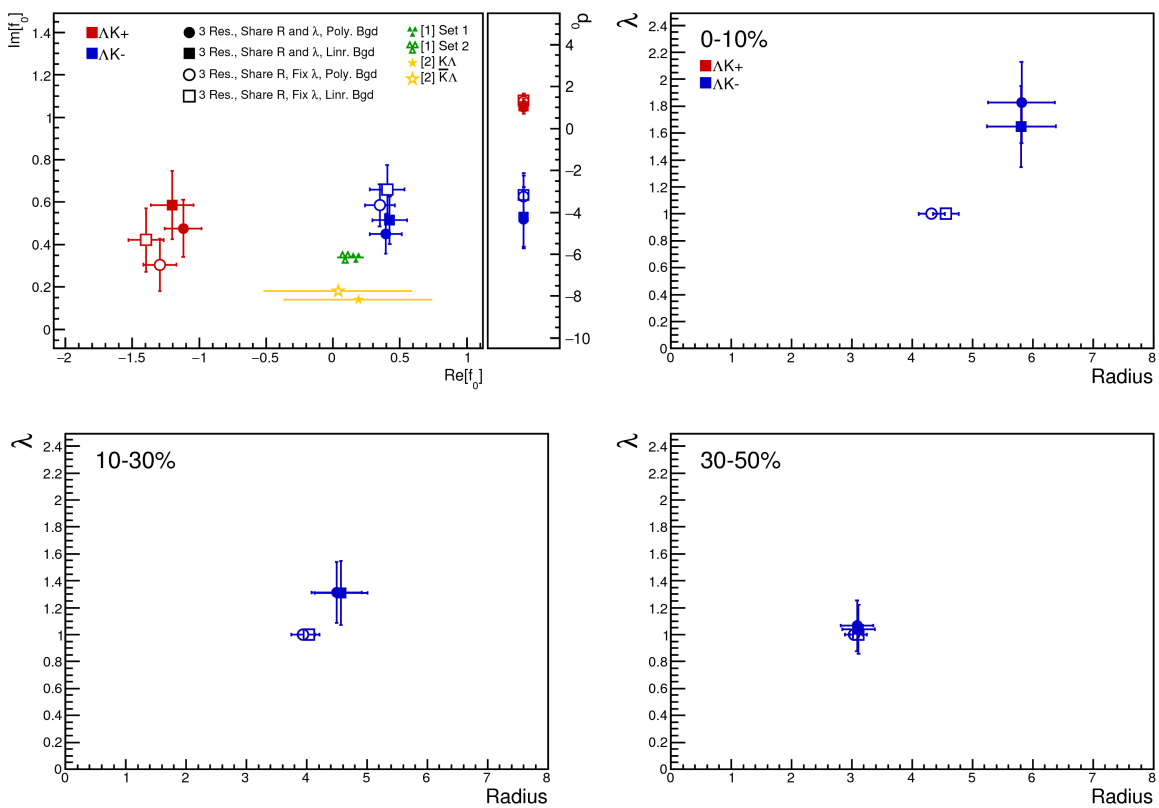


Fig. 20: Compare Fit Parameters: Free vs fixed λ (sharing radii)

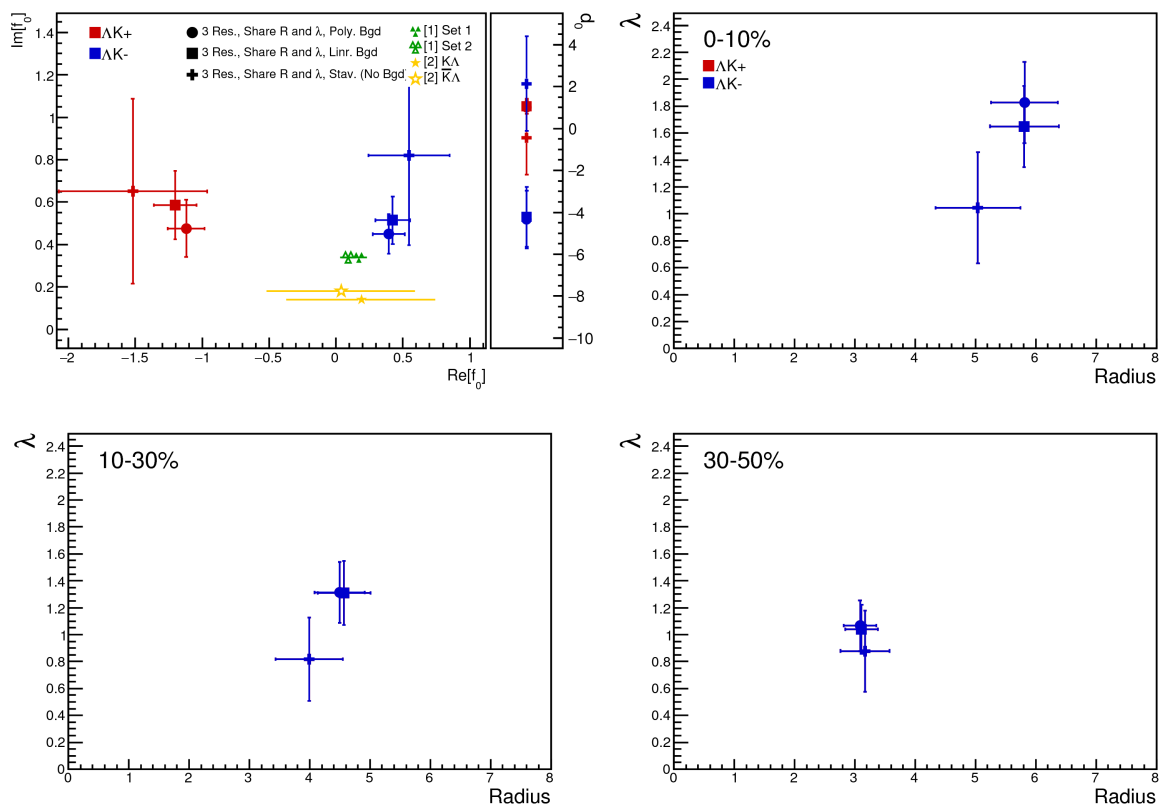


Fig. 21: Compare Fit Parameters: Background methods (sharing radii)

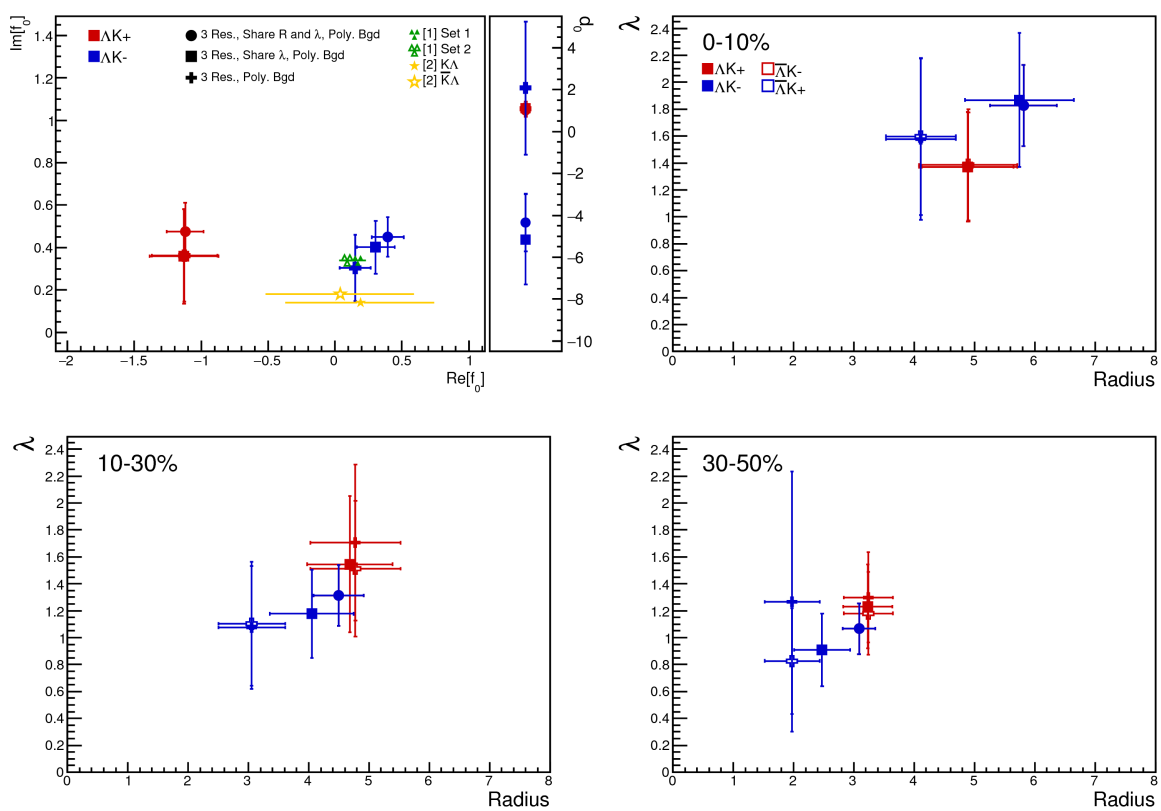


Fig. 22: Compare Fit Parameters: Shared vs. Separate Radii